

# Methods of Robust Snapshot Positioning in Multi-Antenna Systems for Inland water Applications

Christoph Lass\*, Daniel Arias Medina<sup>†</sup>, Michailas Romanovas<sup>‡</sup>, Iván Herrera-Pinzón<sup>†</sup> and Ralf Ziebold<sup>†</sup>

<sup>\*†</sup>German Aerospace Centre (DLR)

Institute of Communications and Navigation  
Germany, 17235 Neustrelitz, Kalkhorstweg 53

\*Email: Christoph.Lass@dlr.de

<sup>‡</sup>BASELABS GmbH

Germany, 09126, Ebertstraße 10

**Abstract**— As the Global Navigation Satellite Systems (GNSS) are increasingly used as the main source of Positioning, Navigation and Timing (PNT) information for maritime and inland water applications, it becomes of crucial importance to ensure the reliability and the accuracy of the GNSS-based navigation solution for certain challenging environments. The presented work extends the previously reported GPS L1C positioning algorithms using robust estimation framework for the scenarios with multiple separate GNSS antennas. The performance of a robust method suitable for multiple outlier mitigation is compared to one of the robust methods designed for a single antenna. The presented schemes are evaluated using real measurement data from inland water scenario with multiple bridges and a waterway lock. The initial results are encouraging and indicate the scalability of the previously suggested robust GPS positioning schemes for setups with multiple GNSS antennas as well as the potential of the methods to be used in integrated navigation systems.

## I. INTRODUCTION

The Global Navigation Satellite Systems (GNSS) can be considered as the cornerstone and the main information source for Positioning, Navigation and Timing (PNT) data in maritime and inland water navigation systems. It is rather well-known that the classical code-based positioning using an iterated least squares (LS) method lacks robustness. Even a single measurement outlier due to space weather events, multipath, non-line-of-sight (NLOS) or jamming can introduce a gross error in the final position solution. Although several approaches, such as classical Receiver Autonomous Integrity Monitoring (RAIM) techniques, have been designed to perform fault detection and exclusion, the methods are often based on a single fault assumption and therefore could fail when there are multiple simultaneous outliers [1]. Although modifications have been suggested to eliminate multiple failures sequentially [2], the schemes can still fail as the correlations in the test statistics often lead to identification and rejection of the wrong satellite.

Recently, alternative strategies for multiple outlier mitigation have been proposed using methods of robust estimation [1], [3], [4]. Here methods of robust regression are applied

to improve the performance of the GNSS positioning in non-favorable environments. These methods are often based on checking the consistency of the observations where the influence of the measurements not fitting the underlying functional or stochastic model is reduced compared to those which fit well [5]. Methods of robust regression have a relatively long history [6], [7] with numerous applications for general data analysis [8], [9]. Although being different in implementation details, the suggested methods have demonstrated an improved positioning performance even when multiple pseudorange measurements were affected simultaneously by multipath or NLOS. Unfortunately, most of the works have reported the performance of the methods using simulated data, and often a systematic evaluation of the alternative methods was missing. In the previous work [10], this problem was addressed by systematically evaluating performance of several representative robust schemes using real measurement data from challenging inland water scenarios with high vessel's dynamics.

The presented work provides an extension of the previously reported robust GNSS snapshot positioning schemes for the setup with multiple independent GNSS antennas. The position as well as the attitude of the ship is calculated in a LS ansatz using all separated GNSS antennas in one equation system. This has the advantage that less observations per antenna and in total are needed with respect to snapshot positioning for all antennas separately. The remaining redundant observations could improve the robustness against multipath and NLOS effects. This is especially important for challenging scenarios, e.g. under bridges, where there is a lack of redundancy of the data such that problematic observations cannot be removed.

In many practical applications it is rather common to use GNSS weighting models (GNSS leveraging) within the solution calculation. An additional discussion is provided on the extension of the presented methods for leveraged measurements using carrier-to-noise density ratio (C/N0) information provided by the GNSS receiver.

## II. METHODOLOGY

### A. Single-Antenna approach

The classical method to determine the position based on GNSS is an iterative weighted least squares approach. The three position coordinates  $x_i$  of antenna  $i$  in the ECEF coordinate system and its receiver clock offset  $\delta t_i$  are determined using the following equation for satellite  $j$

$$C_j^i = \|x_j - x_i\| + c_0 \delta t_i. \quad (1)$$

Note that  $C_j^i$  is the corrected code measurement where errors due to the troposphere, ionosphere and the satellite clock offset have already been considered (see section III for further details).  $\|\cdot\|$  is the Euclidean norm and  $c_0$  is the speed of light. At least four independent observations are required to calculate the unknowns  $x_i$  and  $\delta t_i$ .

Expressing (1) as a weighted least squares problem yields

$$\min_{(x_i, \delta t_i) \in \mathbb{R}^3 \times \mathbb{R}} \frac{1}{2} \sum_{j=1}^{n_i} \omega_j^2 (\|x_j - x_i\| + c_0 \delta t_i - C_j^i)^2 \quad (2)$$

with the weights  $\omega_j$  being positive and  $n_i$  being the number of observations for antenna  $i$ .

This minimisation problem can be solved using Taylor series expansion to linearise the problem and applying the iterative Gauss-Newton method. Before different weighting schemes are introduced, the multi-antenna approach will be described in detail.

### B. Multi-Antenna approach

The developed multi-antenna method is based on the extension of the classical Gauss-Newton iterative weighted LS approach (2) for a system with at least three separated GNSS antennas. For the following discussion the number of antennas is assumed to be exactly three due to the measurement equipment on the ship. It is easy to generalise the results for cases with more antennas.

The estimated state consists of three position coordinates  $x$  of a reference point, three clock offsets  $\delta t_i$  of correspondingly three GNSS receivers and the quaternion  $q$  with the norm constraint  $\|q\| = 1$ . This quaternion describes the attitude of the ship in the ECEF coordinate system. The reference point is usually chosen in the neighbourhood of the antennas, e.g. one of the antennas itself or the location of the IMU.

For antenna  $i$  and satellite  $j$  this yields the following equation:

$$C_j^i = \|x_j - (x + R(q)L_i)\| + c_0 \delta t_i. \quad (3)$$

Note that  $R(q)$  is the rotation matrix from the body framework to the ECEF coordinate system implied by the attitude quaternion, and  $L_i := x_i - x$  is the known lever arm of the reference point  $x$  to the position  $x_i$  of antenna  $i$  in the body framework. The other variables retain their meaning from (1).

At least nine code measurements are required to calculate the unknowns since  $(x, \delta t, q) \in \mathbb{R}^3 \times \mathbb{R}^3 \times \mathbb{R}^4$  and due to the norm constraint of the quaternion. Note that the number of required observations can even be smaller for a receiver with

multiple antennas where only one receiver clock offset has to be determined. This is an advantage over the single-antenna approach which requires at least four observations per antenna, so twelve observations in total for three antennas.

To put (3) in a weighted least squares context, the function  $f_k$  is defined as

$$f_k(x, \delta t, q) := \|x_j - (x + R(q)L_i)\| + c_0 \delta t_i - C_j^i \quad (4)$$

which implies the weighted least squares problem

$$\min_{\substack{(x, \delta t, q) \in \mathbb{R}^3 \times \mathbb{R}^3 \times \mathbb{R}^4 \\ \|q\|=1}} \frac{1}{2} \sum_{k=1}^n \omega_k^2 f_k^2(x, \delta t, q). \quad (5)$$

with  $n := n_1 + n_2 + n_3$  being the total number of observations for all three antennas.

Special care is taken in preserving the norm constraint of the attitude quaternion by using the exponential mapping function [11]

$$\begin{aligned} \exp : \mathbb{R}^3 &\rightarrow \{q \in \mathbb{R}^4 : \|q\| = 1\} \\ \exp(w) &:= \begin{cases} \left( \cos(\|w\|), \sin(\|w\|) \frac{w}{\|w\|} \right)^\top & w \neq 0_3 \\ (1, 0, 0, 0)^\top & w = 0_3 \end{cases} \quad (6) \end{aligned}$$

instead of the quaternion  $q$ . This yields the following weighted least squares problem which is equivalent to (5):

$$\begin{aligned} \min_{(x, \delta t, w) \in \mathbb{R}^3 \times \mathbb{R}^3 \times \mathbb{R}^3} \frac{1}{2} \sum_{k=1}^n \omega_k^2 f_k^2(x, \delta t, \exp(w)) &\quad (7) \\ = \min_{(x, \delta t, w) \in \mathbb{R}^3 \times \mathbb{R}^3 \times \mathbb{R}^3} F(x, \delta t, \exp(w)) \end{aligned}$$

Note that this formulation makes it easier to see why nine observations can suffice. The minimisation problem (7) is solved by linearising  $f_k$  using Taylor series expansion and using the modified Gauss-Newton method where the additive updates in each iteration are damped by using  $\lambda \in (0, 1]$  with

$$\begin{aligned} F^{(l+1)}(\lambda) &:= F\left(x^{(l)} + \lambda \Delta x, \delta t^{(l)} + \lambda \Delta \delta t, w^{(l)} + \lambda \Delta w\right) \\ M &:= \left\{ \lambda \in \left\{ 1, \frac{1}{2}, \frac{1}{4}, \frac{1}{8} \right\} : F^{(l+1)}(\lambda) < F^{(l+1)}(0) \right\} \\ \lambda &= \begin{cases} \frac{1}{8} & M = \emptyset \\ \max M & \text{else} \end{cases} \end{aligned}$$

This is done to avoid the convergence issues since the Gauss-Newton method is known to only converge locally, and it can make large updates which deviate from the root. Note that  $w$  is actually not used between different iterations but a multiplicative quaternion update is done which is known to preserve the norm of unit quaternions.

$$\begin{aligned} \exp\left(w^{(l+1)}\right) &= q^{(l+1)} = \exp(0_3) \otimes q^{(l+1)} \\ &= \exp(\delta w) \otimes q^{(l)} \end{aligned}$$

In each iteration  $\delta w$  is calculated and used to update to attitude quaternion. This multiplicative update has to be

considered when determining the derivative of  $f_k$  with respect to  $\delta w$ :

$$D_{\delta w} f_k(x, \delta t, \exp(\delta w) \otimes q) \Big|_{\delta w=0_3} \\ = D_q f_k(x, \delta t, q) \begin{pmatrix} -q_2 & -q_3 & -q_4 \\ q_1 & q_4 & -q_3 \\ -q_4 & q_1 & q_2 \\ q_3 & -q_2 & q_1 \end{pmatrix}.$$

### C. Weighting schemes

Three different weighting schemes with regard to the satellites were applied to  $\omega_k$ :

#### 1) Elevation angle $\theta$ (EA)

It has been proven that the possible errors of the observed pseudoranges increase with low elevation satellites [12]. As the navigation message covers a longer distance through the ionosphere layer, it is deeply affected. Furthermore, the signals are more likely to get reflected compared to the signal coming from a satellite with a high elevation.

$$\frac{1}{\omega_k^2} = \frac{1}{\sin^2(\theta_i)} \quad (8)$$

#### 2) Carrier-to-noise ratio (C/N0)

Carrier-to-noise ratio is a measure of signal strength and represents current signal power conditions.

$$\frac{1}{\omega_k^2} = a + b \cdot 10^{-\frac{C/N_0 - c}{10}} \quad (9)$$

The parameters are chosen according to the environment and the user equipment. For this measurement campaign, the parameters were found as  $a = 0.60006$ ,  $b = 50.63920$  and  $c = 33.83850$  as a result of a regression problem.

#### 3) Equal weights for all satellites (N)

### D. Robust methods

The classical least squares method is quite sensitive to outliers as one single outlier can drive to aberrant gross errors in the estimation solution [13]. A robust alternative proposed by many authors is to change the function to be minimised, i.e. Edgeworth [14] introduced the last absolute values or  $L_1$  criterion as

$$\min_x \sum_{k=1}^n |f_k(x)|. \quad (10)$$

Despite the  $L_1$  criterion offering some additional protection against outlying observations, this method yields the same disadvantage as the classical LS method since one outlier can heavily disturb the estimated solution. For the measurement data analysed in this paper, the iteratively reweighted least squares (IRLS) method was used.

The procedures based on IRLS use the whole set of observations to compute a solution for the minimisation problem. Then the residuals of the observations are used to adapt the weights such that observations having large residuals are

down weighted and vice versa for observations having small residuals. According to [15] the IRLS algorithm has only first degree convergence and needs a good initial estimate to have a fast convergence.

The generalised M estimators (GM-estimators) proposed by Mallows [16] are used to recompute the weights. The leverage of the observations are based on the *reliability number* [7], a parameter which combines the prior knowledge of the measurement uncertainty with its influence on the geometry matrix  $G$  of the solution as

$$T = R^{-1} - G (G^T R G)^{-1} G^T \quad (11)$$

where  $R = \text{diag}[\sigma_1^2, \dots, \sigma_n^2]$  corresponds to the covariance matrix of the measurements. The weighting schemes from subsection C were used for this, i.e.

$$\sigma_i^2 = \frac{1}{\omega_i^2}. \quad (12)$$

The matrix  $T$  is denoted as the cofactor matrix by various authors, cf. [3], [17], and it is used to determine the reliability number  $g_i$  of each measurement which is defined as

$$g_i := \left( \sqrt{TR} \right)_{i,i}. \quad (13)$$

The indexing  $(\cdot)_{i,i}$  stands for the entries on the diagonal of the matrix. The reliability number is only valid for GM-estimators when the observations are uncorrelated [3]. The weighting function in the IRLS method becomes

$$w_i := \begin{cases} g_i & g_i \frac{|r_i|}{\hat{\sigma}} \leq c \\ c g_i \frac{\hat{\sigma}}{|r_i|} & g_i \frac{|r_i|}{\hat{\sigma}} > c \end{cases} \quad (14)$$

with  $c = 1.345$  and the scaling factor  $\hat{\sigma}$  being chosen as the median absolute deviation of the residuals  $r = (r_1, \dots, r_n)$ , that is

$$\hat{\sigma} := 1.48 \text{med}(|r - \text{med}(r)|). \quad (15)$$

Other well known robust estimators are the least median of squares [13], the M estimator developed by Huber [6] or the S estimator proposed by Rousseeuw and Yohai [18].

## III. MEASUREMENT CAMPAIGN

The performance of the developed methods has been evaluated using real observations from the measurement campaign conducted on 25th March 2014 (DOY 084, UTC 13:00-14:00) near Koblenz (Germany) on the Moselle river. The demonstration area covers several challenging scenarios for inland water navigation, as can be seen in Figure 1. Sailing downstream, a lock bounds the measurement area three kilometers before the confluence with Rhine river. After the lock, three bridges of different height and width span the river in a relatively short section ((B) and (C) in Fig. 1) of only two kilometers. This is making a reliable and continuous positioning using pure GNSS information rather challenging. The first bridge starting from the west is the tallest 4-lane car bridge ‘‘Europabruecke’’ with a width of 40 meters and clearance height of 13.9 meters. The next bridge is the railway bridge which is 25 meters wide with

a low clearance of only 10.2 meters and oval clearance profile. The last one is the “Balduinbruecke” with a width of 10 meters and a height of 12.1 meters. Therefore, it is relatively small in comparison to the other two.

The vessel performed an 8-shaped trajectory (total duration 1 hour) with two passes under these bridges and the waterway lock in order to ensure that the GNSS signals are strongly affected by the shadowing from bridges and other obstacles.

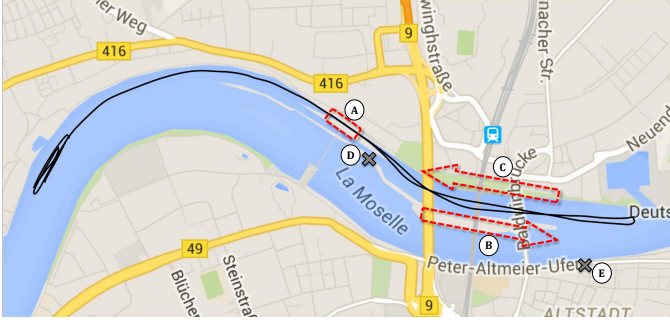


Fig. 1. Measurement area on the river Moselle near Koblenz (Germany). Reference path (black line) and several challenging segments including the lock (A), and 3-bridge segments (B) and (C). Geodetic total stations (D) and (E)

The sensor system onboard the research vessel “MS Bingen” (see Fig. 2) consisted of three geodetic GNSS antennas and Javad Delta receivers. The distance between the three GNSS antennas is 3.99 respectively 13.55 meters. The ionosphere propagation delay corrections have been applied using the classical Klobuchar model. The corresponding troposphere corrections are based on the Saastamoinen model in order for the results to be representative for user equipment without ground-based correction information [19]. No elevation mask for GNSS satellites has been used as to ensure the best possible availability of the GNSS measurements.



Fig. 2. Research vessel “MS Bingen” used in the measurement campaign and the corresponding measurement equipment

In order to accurately track the position of the vessel without depending on GNSS information, two geodetic total stations have been placed on the shores of the river (see (D) and (E) in Figure 1). As the total stations combine the use of angle and distance measurements in order to determine only the horizontal position, the vertical accuracy is not addressed in this report. The coordinates of the tracked object are given

relative to a known reference point and are determined using trigonometry and triangulation as long as a direct line of sight (LOS) is maintained between the two points. With the use of two total stations the availability of the reference trajectory is ensured even in the problematic areas where GNSS failed. After the reference 1 Hz position information is obtained, the post-processing and adjustment of the measurements ensure an accuracy of less than 2 cm for the presented evaluation path.

#### IV. RESULTS

In the following discussion the solver prematurely terminates when either the Gauss-Newton method reaches 100 iterations or  $\|\Delta x\|, \|\Delta c_0 \delta t\| < 1$  mm as well as  $\|\delta w\| < 10^{-3}$ . For the multi-antenna approach described in subsection II-B, antenna three has been chosen as the reference point, that is  $x = x_3$  in (3) which is located midship (see Figure 2). This is compared to the solution of the single-antenna approach from II-A with regard to antenna three. At first the quality of the positioning will be analysed in the next two subsections. The calculation of the attitude via the quaternion is discussed in a separate subsection.

##### A. Non-robust methods

The discussion starts with the non-robust methods where the horizontal positioning is compared between the different approaches and weights with respect to the ground truth calculated by the two total stations at the river Moselle. The following figure shows the results for the C/N0 weighting scheme.

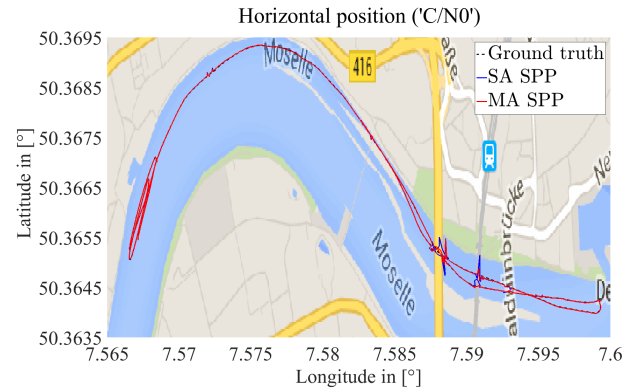


Fig. 3. Horizontal position of single- and multi-antenna approach using the C/N0 weighting scheme without GM-estimator

The overall horizontal position is tracked well, i.e. the mean horizontal position error (HPE) is less than 3 meters which is under the specifications of GPS L1. There is little difference between the two approaches in the mean as the ground truth can hardly be seen in this figure. The largest outliers happen during the passing of the ‘Europabruecke’ and the railway bridge while the ‘Balduinbruecke’ seems to cause little errors. The same goes for the waterway lock which has little effect on the precision of the horizontal positioning. The passing of

the bridges will be looked on in more detail later. In order to make a more thorough analysis the HPE will be presented in numerical values.

In the following tables the HPE is given in the mean, the maximum and the root mean square (RMS) as well as the percentage of cases where the solver was terminating before the maximum number of iterations was reached, e.g. 100.

TABLE I

HPE AND CONVERGENCE USING DIFFERENT ANTENNA APPROACHES AND WEIGHTING SCHEMES WITHOUT GM-ESTIMATOR

Approach	Weighting scheme	HPE in [m]			Convergence in [%]
		Max	Mean	RMS	
Single	N	50.70	2.89	4.53	100.00
Multi	N	47.61	2.75	4.17	97.50
Single	EA	91.79	1.70	4.15	100.00
Multi	EA	45.49	1.73	3.32	95.69
Single	C/N0	49.32	1.47	2.84	100.00
Multi	C/N0	43.35	1.32	2.31	98.61

The good determination of the horizontal position in the mean is confirmed by the above table for the schemes using different weights with regard to the observation of the satellites. Overall the C/N0 weighting scheme produces the best results for this measurement scenario though the difference to the elevation angle scheme is only in the decimeter regime. Note that the single-antenna approach causes a HPE of over 90 meters which does not happen with the multi-antenna approach. This shows that the additional redundancy in the number of required observations helps with increasing the accuracy of the positioning. Also the multi-antenna approach has the best results for all weighting schemes with the small exception being the mean of the EA scheme.

A disadvantage of the multi-antenna scheme is the number of iterations needed to converge as the single-antenna approach only needed about five iterations in the mean to converge. This is in contrast to the multi-antenna scheme which needed about 20, 32 respectively 34 (N, EA and C/N0 weights) iterations in the mean to converge which is still small enough to ensure real-time computation capability. Note that the multi-antenna approach did not converge in all cases but this can be fixed by choosing a larger number of maximum iterations and allowing a smaller  $\lambda$  in the modified Gauss-Newton method. To make a fair comparison to the results of the robust method with regard to the computation time the parameters were chosen as described in the beginning of this section.

Before the results of the robust method are analysed, a closer look is taken at the horizontal positioning during the passing of the three bridges where the largest HPE occurred.

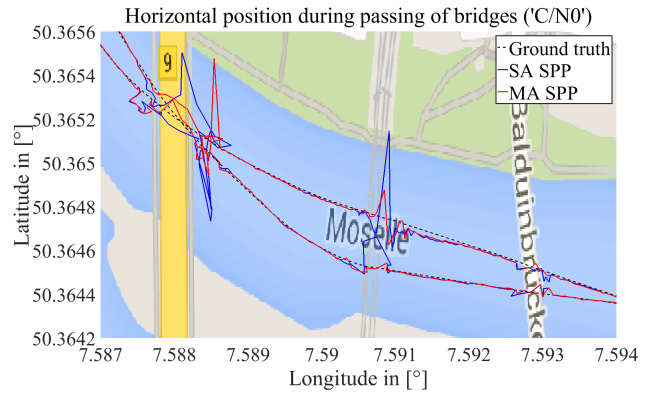


Fig. 4. Horizontal position of single- and multi-antenna approach using the C/N0 weighting scheme without GM-estimator during passing of bridges

The above figure confirms that the largest horizontal positioning errors occur during the passing of ‘Europabruecke’ as well as the railway bridge while the ‘Balduinbruecke’ causes little deviations. What is interesting to see is that the multi-antenna approach in contrast to the single-antenna scheme handles the railway bridge quite well. Also the multi-antenna results only have one large outlier with an HPE of over 40 meters at the ‘Europabruecke’ where as the single-antenna approach has two of them there.

Overall the multi-antenna approach provides a more accurate positioning in the mean as well as in the worst cases where the largest HPE occurs and is therefore more reliable when using non-robust method for this measurement campaign.

### B. Robust methods

The discussion of the robust method starts with the following table presenting the numerical values of the horizontal positioning which later will be compared in a separate table to the non-robust results.

TABLE II

HPE AND CONVERGENCE USING DIFFERENT ANTENNA APPROACHES AND WEIGHTING SCHEMES WITH GM-ESTIMATOR

Approach	Weighting scheme	HPE in [m]			Convergence in [%]
		Max	Mean	RMS	
Single	N	40.55	2.29	3.23	29.47
Multi	N	32.99	2.20	2.93	18.08
Single	EA	113.66	1.83	3.94	49.17
Multi	EA	46.16	1.82	2.94	26.00
Single	C/N0	48.86	1.70	2.84	43.53
Multi	C/N0	38.96	1.81	2.66	21.50

Again the multi-antenna approach delivers the best results. The maximum HPE is reduced by the robust method with the EA weighting scheme being an exception for both approaches. Note that the mean and RMS HPE actually decrease for N and partially the EA scheme where as the C/N0 weighting scheme has worse results in comparison to the non-robust results though it’s better than the other weighting schemes using the GM-estimator.

A problem of the robust method used here is the low number of cases where convergence occurred which is even worse

for the multi-antenna approach. While this is of concern it has to be noted that for non-converging cases the weights cycle between two to four different states in the end which only differ in the mean by 20.5 cm for the single-antenna and 3.8 cm for the multi-antenna approach. So there is little difference in the horizontal position between the iterations where the weights switch between different states. But it has to be mentioned that there were five cases for the multi-antenna scheme where the horizontal position changed by over one meter though this didn't affect the maximum absolute HPE.

One way to improve the convergence could be to not change the weights every iteration but only after the position for one set of weights converged. This is then compared to the fixed position of the previous weights in an outer loop to decide whether the weights have to be changed again. Furthermore, other robust methods have to be tested which have less strict requirements than the GM-estimator. For instance, the observations of the multi-antenna scheme cannot be without correlation.

The following figure shows the horizontal position during the passing of the bridges which has the largest HPE.

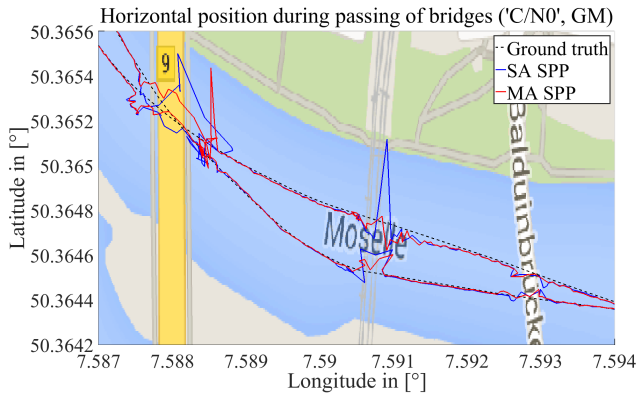


Fig. 5. Horizontal position of single- and multi-antenna approach using the C/N0 weighting scheme with GM-estimator during passing of bridges

With regard to Figure 4 one can see the most improvements for the single-antenna approach at the 'Europabruecke' where only one sample has a HPE larger than 40 meters. Nonetheless the single-antenna scheme fails again under the railway bridge where as the multi-antenna approach provides a more accurate positioning. For both schemes the 'Balduinbruecke' causes little problems which was also the case for the non-robust calculations. Note that the robust methods slightly deviate more from the ground truth between the bridges. This can also be seen by the mean and RMS error in the following table which compares the non-robust to the robust methods using the equal weighting scheme. This scheme was chosen as it showed the most improvements using the GM-estimator.

TABLE III  
HPE AND CONVERGENCE USING DIFFERENT ANTENNA APPROACHES WITH AND WITHOUT GM-ESTIMATOR USING EQUAL WEIGHTING SCHEME

Approach	Robust method	HPE in [m]			Convergence in [%]
		Max	Mean	RMS	
Single	–	50.70	2.89	4.53	100.00
Single	GM-estimator	40.55	2.29	3.23	29.47
Multi	–	47.61	2.75	4.17	97.50
Multi	GM-estimator	32.99	2.20	2.93	18.08

One can clearly see that using the GM-estimator reduces the maximum, mean and RMS horizontal positioning error. This is not the case for the other weighting schemes as the a priori knowledge of the observations' quality is misleading during periods of NLOS or multipath. Furthermore, the multi-antenna approach is clearly superior to the single-antenna approach since it lessens the maximum HPE by at least three meters and improves the mean as well as the RMS HPE.

In contrast to the non-robust methods, increasing the maximum number of iterations or allowing a smaller  $\lambda$  did not significantly improve the number of samples with convergence. This only lengthened the computation time for the multi-antenna scheme.

To sum it up, the multi-antenna approach improves the accuracy of the horizontal positioning with little regards to the chosen weighting scheme with and without using a robust method. The GM-estimator caused convergence issues for both approaches though the actual difference between the positions calculated for non-converging samples during the iterations are of little significance with respect to the actual HPE. Still, there are ways to improve the convergence to ensure reliable positioning which should be tested using the multi-antenna approach.

### C. Quality of attitude quaternion

For the last subsection the attitude quaternions computed by the multi-antenna approach are discussed. As there was little difference between the weighting schemes and the used robust method, only the C/N0 weighting scheme without using the GM-estimator is analysed here.

The following figure shows the Euler angles derived from the quaternion for the first six minutes. Note that during that period there were with no high structures around the measurement area which could cause unwanted effects such as multipath or NLOS. Note that the radius in the figure represents the time of the sample.

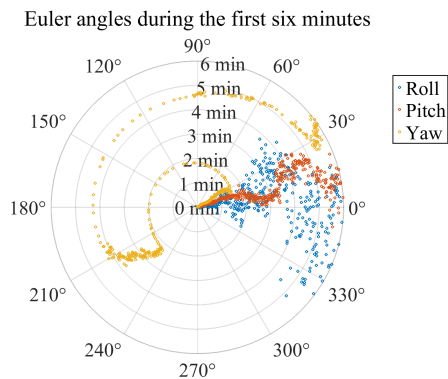


Fig. 6. Euler angles during the first six minutes

The multi-antenna approach shows a good estimation of the attitude of the ship. Roll varies the most, that is by about  $\pm 30$  degrees which is to be expected since the two GNSS antennas at the back of the ship are only four meters apart and the mean HPE is larger than one meter. Pitch has smaller variance with the largest deviations being during the sixth minute. Yaw seems to be the most reliable angle and only has little variance which implies a reliable heading. Of course, this has to be confirmed by the compass data which unfortunately could not be analysed for this measurement campaign.

In contrast to the figures of the previous subsections, a closer look is now taken at the passing of the waterway lock. The figure below shows the Euler angles during that period of time.

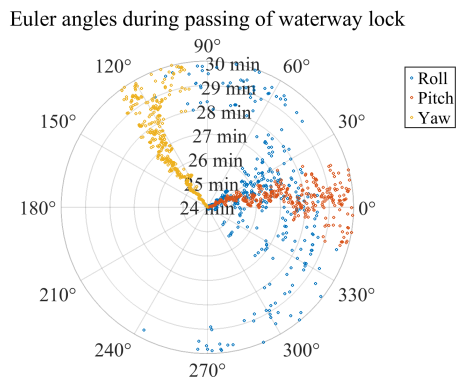


Fig. 7. Euler angles during passing of waterway lock (between minutes 24 and 30)

One can see that only two Euler angles only seem to be reliable with pitch and yaw having increased variance starting from minute 28. Roll is unpredictable during the passing of the waterway lock. The same phenomena occurs during the passing of the bridges where even pitch and yaw are unreliable. This suggests that the precision of the attitude quaternion is heavily affected by multipath and NLOS.

These initial results indicate that for a reliable calculation of the attitude using the multi-antenna approach either the distance of the antennas must be sufficiently large or that

only environments with little to no obstructions can be used to determine the Euler angles.

## V. SUMMARY & OUTLOOK

The work presented a multi-antenna GNSS approach where the position, the receiver clock offsets as well as the attitude of a ship with at least three independent GNSS antennas are calculated in one IRLS scheme. The mathematical framework as well as a short explanation of the numerical methods used were described in section II. The developed methods were tested with real measurement data using different weighting schemes. The results looked promising with the multi-antenna approach having better results than the single-antenna approach. The robust method used caused convergence issues with little disturbance on the positioning. Nonetheless, the robust method helped to reduce the maximum absolute error.

What is still unclear is whether the convergence issues were caused by the numerical methods or the measurement data itself. To test this it is planned to apply the multi-antenna approach to different data sets with better conditions that is less obstructing environment to avoid effects such as NLOS or multipath and with larger distance between the antennas on the ship to increase the quality of the quaternion calculation. Furthermore the latter has to be verified using an independent measurement such as IMU and compass data.

Another way to reduce the maximum error is to combine the positioning data calculated by the multi-antenna scheme with inertial data in a sensor fusion approach, i.e. using an extended or unscented Kalman filter. Other interesting topics are the multi-antenna observability, the interpretation of the Jacobian as the geometry matrix and the related dilution of precision (DOP) to predict larger positioning errors.

## REFERENCES

- [1] J. Wang and J. Wang, "Mitigating the effect of multiple outliers on GNSS navigation with M-estimation schemes," in *International Global Navigation Satellite Systems Society IGSS Symposium*, The University of New South Wales, Sydney, Australia, 4-6 December 2007.
- [2] H. Kuusniemi, G. Lachapelle, and J. Takala, "Reliability in personal positioning," in *Proceedings of GNSS 2004 Conference*, Rotterdam, 16-19 May 2004.
- [3] N. L. Knight and J. Wang, "A comparison of outlier detection procedures and robust estimation methods in GPS positioning," *Journal of Navigation*, vol. 62, pp. 699-709, 10 2009.
- [4] P. D. Groves and Z. Jiang, "Height Aiding,  $C/N_0$  weighting and consistency checking for GNSS NLOS and multipath mitigation in urban areas," *The Journal of Navigation*, vol. 66, no. 653-669, 2013.
- [5] A. Wieser and F. K. Brunner, "Short static GPS sessions: Robust estimation results," *GPS Solutions*, vol. 5, no. 3, pp. 70-79, 2002. [Online]. Available: <http://dx.doi.org/10.1007/PL00012901>
- [6] P. J. Huber, "Robust regression: asymptotics, conjectures and Monte Carlo," *The Annals of Statistics*, pp. 799-821, 1973.
- [7] K.-R. Koch, *Parameter estimation and hypothesis testing in linear models*. Springer Science & Business Media, 1999.
- [8] D. L. Massart, L. Kaufman, P. J. Rousseeuw, and A. Leroy, "Least median of squares: a robust method for outlier and model error detection in regression and calibration," *Analytica Chimica Acta*, vol. 187, pp. 171 - 179, 1986.
- [9] Y. Susanti, H. Pratiwi, S. Sulistijowati, and T. Liana, "M estimation, S estimation, and MM estimation in robust regression," *International Journal of Pure and Applied Mathematics*, vol. 91, no. 3, pp. 349-360, November 2014.

- [10] D. A. Medina, M. Romanovas, I. D. Herrera Pinzon, and R. Ziebold, "Robust position and velocity estimation methods in integrated navigation systems for inland water applications," in *IEEE/ION Position Location and Navigation Symposium (ION PLANS)*, 2016.
- [11] A. Ude, "Nonlinear least squares optimisation of unit quaternion functions for pose estimation from corresponding features," in *14th International Conference on Pattern Recognition, Brisbane, Australia*, August 1998, pp. 425–427.
- [12] J. Wang, M. P. Stewart, and M. Tsakiri, "Stochastic modeling for static gps baseline data processing," *Journal of Surveying Engineering*, vol. 124, no. 4, pp. 171–181, 1998.
- [13] P. J. Rousseeuw, "Least median of squares regression," *Journal of the American Statistical Association*, vol. 79, no. 388, pp. 871–880, 1984.
- [14] F. Y. Edgeworth, "On observations relating to several quantities," *Hermathena*, vol. 6, no. 13, pp. 279–285, 1887.
- [15] H. Pesonen, "Robust estimation techniques for GNSS positioning," in *NAV07 - Navigation Conference and Exhibition*, Longen, England, 31.10 - 1.11 2007, pp. 1–7.
- [16] C. L. Mallows, "On some topics in robustness," *Unpublished memorandum, Bell Telephone Laboratories, Murray Hill, NJ*, 1975.
- [17] H. Kuusniemi, A. Wieser, G. Lachapelle, and J. Takala, "User-level reliability monitoring in urban personal satellite-navigation," *Aerospace and Electronic Systems, IEEE Transactions on*, vol. 43, no. 4, pp. 1305–1318, 2007.
- [18] P. Rousseeuw and V. Yohai, "Robust regression by means of S-estimators," in *Robust and nonlinear time series analysis*. Springer, 1984, pp. 256–272.
- [19] K. Borre and G. Strang, *Algorithms for Global Positioning*. Wellesley-Cambridge Press, 2010.